Half-metallic properties of $Co_2(Cr_{1-x}Fe_x)Ga$ Heusler alloys

R. Y. Umetsu,*,† K. Kobayashi,* A. Fujita, K. Oikawa,* R. Kainuma,* and K. Ishida*
Department of Materials Science, Graduate School of Engineering, Tohoku University, Aoba 6-6-02, Sendai, 980-8579, Japan

N. Endo and K. Fukamichi
Institute of Multidisciplinary Research for Advanced Materials, Tohoku University, Katahira 2-1-1, Sendai, 980-8577, Japan

A. Sakuma
Department of Applied Physics, Graduate School of Engineering, Tohoku University, Aoba 6-6-08, Sendai, 980-8579, Japan
(Received 26 January 2005; revised manuscript received 22 September 2005; published 8 December 2005)

Magnetic and half-metallic properties of $Co_2(Cr_{1-x}Fe_x)Ga$ Heusler alloys have been investigated. In the entire concentration range, the $L2_1$-type ordered phase is obtained. The saturation magnetic moment M_s at 4.2 K for $x=0.0$ ($\equiv Co_2CrGa$) is $3.01\mu_B$/f.u., in agreement with the generalized Slater-Pauling line and consistent with the theoretical value. The experimental value of M_s increases with increasing x, slightly larger than that of the theoretical value above $x=0.60$. The Curie temperature T_C also increases with x, and qualitatively accords with the theoretical values estimated from the effective exchange constant J_0. The present theoretical results disclose that not only the $L2_1$-type ordered phase but also the $B2$-type phase exhibits high values of the spin polarization ratio P in a low concentration range of x. The ratio P of the $L2_1$- and $B2$-type phases decreases with increasing x, because the large peak of the density of states at the Fermi energy for Cr in the majority spin band becomes smaller and a strong hybridization between Co-3d and Fe-3d makes a gap narrower in the minority spin band.

DOI: 10.1103/PhysRevB.72.214412 PACS number(s): 75.30.Cr, 75.50.Cc, 71.20.Be

I. INTRODUCTION

Half-metallic ferromagnets (HMFs) with a high spin polarization ratio have been investigated intensively in fields of spintronics because magnetic tunnel junctions (MTJs) consisting of HMFs are expected to have a large tunnel magneto-resistance (TMR). Therefore, they are considered to be promising candidates for spintronic devices such as the magnetic random access memories (MRAMs) and magnetic sensors.[1] From band calculations, it has been first pointed out by de Groot *et al.* that the spin polarization ratio in the density of states (DOSs) for $C1_b$ (half-Heusler)-type alloys of NiMnSb and PtMnSb is 100%.[2] Subsequently, electronic structures of $L2_1$ (full-Heusler)-type various HMFs have been calculated and experimental investigations have been made from the practical viewpoints.[3–8] The $L2_1$ and $B2$-type phases of Co_2CrAl alloys have also been reported to exhibit a characteristic evidence of HMFs in their DOSs.[9–12] However, the saturation magnetic moment of the $B2$-type Co_2CrAl alloy is significantly smaller than the theoretical value.[13] For the study of MTJs in $Co_2(Cr_{1-x}Fe_x)Al$ alloy system, moreover, it has been reported that the spin polarization ratio P estimated from using Julliére's model and the TMR ratio of $x=0.40$ are rather higher than those of $x=0.0$.[14] This behavior contradicts the theoretical results that the ratio of P decreases with increasing x for the $L2_1$- and $B2$-type phases of $Co_2(Cr_{1-x}Fe_x)Al$ alloy system.[14] Recently, it has been verified that an inevitable two-phase separation due to a spinodal decomposition occurs in a low concentration range of x and results in a significant reduction of the half-metallic properties.[15] The thermodynamical calculations reveal that the equilibrium two phases are CoAl-rich $B2$ phase and the CoCr-rich $A2$ phase.[16] It has been reported that the phase stability of the $B2$ phase in a bulk specimen is enhanced with increasing of x and a single phase of $B2$-type is obtainable more than $x=0.40$.[15]

In our previous experimental and theoretical investigations, it has been demonstrated that the experimental value of the saturation magnetic moment M_s of the $L2_1$-type ordered Co_2CrGa alloy coincides with the theoretical value, and both the $L2_1$ and $B2$ phases of Co_2CrGa exhibit a half-metallic behavior in their electronic structures.[17] Comparing the phase diagram of Co-Cr-Ga (Ref. 18) with that of Co-Cr-Al (Ref. 19) ternary alloy systems, the single phase of $B2$ region in the former is much wider than that in the latter. Therefore, in light of phase stability, the two-phase separation due to the spinodal decomposition would not occur, and hence, Co_2CrGa alloy is expected to be more practical. For applications, it is also very important to exhibit a high Curie temperature T_C as well as high value of P because the high TMR ratio should be kept above room temperature. The value of T_C for the $L2_1$-type ordered Co_2CrGa alloy has been reported to be 495 K.[17] The partial substitution of Fe for Cr is expected to enhance the Curie temperature in analogy with the $Co_2(Cr_{1-x}Fe_x)Al$ alloy system.[15] In the present study, we have investigated the magnetic and half-metallic properties of both the $L2_1$- and $B2$-type phases for the $Co_2(Cr_{1-x}Fe_x)Ga$ alloy system.

II. EXPERIMENT

The specimens were made by melting in an induction furnace in an argon gas atmosphere and annealed at 1373 K for 72 hours, and quenched into ice water. The alloy with

$x=0.0$ ($\equiv Co_2CrGa$) was additionally annealed at 973 K for 1 week for comparison. The compositions of the samples were confirmed with an electron probe microanalyzer, and the deviation from the stoichiometric composition was less than 1%. The microstructural observations were carried out with an optical microscope. The crystal structure of the specimens was identified as the $L2_1$-type by x-ray powder diffraction (XRD) and transmission electron microscopy (TEM). The magnetic measurements were made with a superconducting quantum interference device (SQUID) magnetometer and a vibrating sample magnetometer (VSM). The Curie temperature was determined by differential scanning calorimetry (DSC) and VSM measurements.

III. MORPHOLOGY OF THEORETICAL CALCULATIONS

The linear muffin-tin orbital (LMTO) method combined with the atomic sphere approximation (ASA) was used within the framework of the local spin density (LSD) functional approximation.[20–22] The coherent potential approximation (CPA) was complemented for the calculation of the $B2$-type phase. In the LMTO scheme, the effective exchange constant J_0 is given by the following expression:[23,24]

$$J_0 = -\frac{1}{4\pi}\,\mathrm{Im}\int^{E_F} d\omega\,\mathrm{Tr}_{lm}[\Omega_0(\omega)\{g^{\gamma_{00}^{\uparrow\uparrow}}(\omega) - g^{\gamma_{00}^{\downarrow\downarrow}}(\omega)\} + \Omega_0(\omega)g^{\gamma_{00}^{\uparrow\uparrow}}(\omega)\Omega_0(\omega)g^{\gamma_{00}^{\downarrow\downarrow}}(\omega)], \quad (1)$$

where $g(\omega)$ is the so-called auxiliary Green function given by $g^{\sigma\sigma'}(\omega)=[(p(\omega)-S)^{-1}]_{ij}^{\sigma\sigma'}$ which constitutes the potential function $p^{\gamma}(\omega)$ and the structure constant S defined in the LMTO method, and Ω_i is given as $\Omega_i(\omega)\equiv\{p_i^{\uparrow}(\omega)-p_i^{\downarrow}(\omega)\}$. The potential function $p^{\gamma}(\omega)$ can be determined self-consistently within the LSD functional approximation. In Eq. (1), Tr stands for the trace over the orbital (l,m), and the integration is performed up to the Fermi energy E_F. If one refers to the classical Heisenberg model, the Hamiltonian is given by $H=-\Sigma_{i,j}J_{ij}\mathbf{e}_i\cdot\mathbf{e}_j$, where $\mathbf{e}_i$ denotes unit vector, J_0 in Eq. (1) corresponds to $J_0=\Sigma_{i\neq 0}J_{i0}$ and then can be regarded as an effective exchange constant, a magnitude of the exchange field, acting on the moment at the 0th site. Hence, we can use J_0 for the estimation of the Curie temperature by adopting the molecular field approximation (MFA) for the spin system by[24]

$$T_C = \frac{2J_0}{3k_B}, \quad (2)$$

where k_B is the Boltzmann constant.

The spin polarization ratio P is computionally given as follows:[25]

$$P(\%) = \left|\frac{N_{\uparrow}(E_F) - N_{\downarrow}(E_F)}{N_{\uparrow}(E_F) + N_{\downarrow}(E_F)}\right| \times 100, \quad (3)$$

where $N_{\uparrow}(E_F)$ and $N_{\uparrow}(E_F)$ denote the density of states (DOSs) at the Fermi energy E_F of the majority spin state and the minority spin state, respectively.

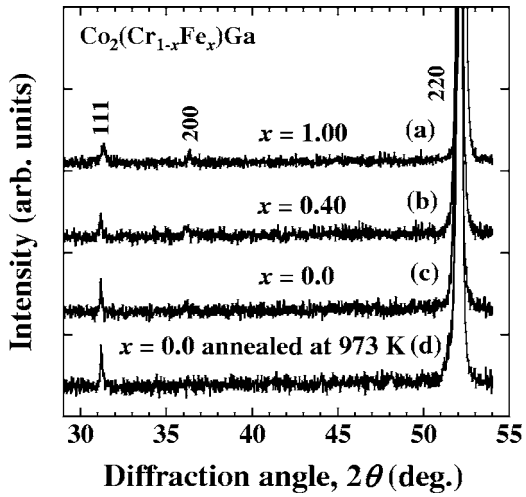

FIG. 1. X-ray diffraction patterns for $Co_2(Cr_{1-x}Fe_x)Ga$ alloys by using Co$K\alpha$ radiation. (a), (b), and (c) are the XRD patterns for $x=0.0$, 0.40, and 1.00 quenched from 1373 K, respectively. (d) is for $x=0.0$ annealed at 973 K for 1 week after quenching from 1373 K.

IV. RESULTS AND DISCUSSION

Figures 1(a)–1(c) show the room temperature x-ray diffraction (XRD) patterns by using Co$K\alpha$ radiation for $Co_2(Cr_{1-x}Fe_x)Ga$ alloys with $x=1.00$, 0.40, and 0.0 quenched from 1373 K, respectively. (d) is that with $x=0.0$ annealed at 973 K for 1 week after quenched from 1373 K. The XRD patterns for (a), (b), and (c) are identified as the $L2_1$-type ordered structure, the superlattice diffractions 111 and 200 can be observed. The ordering between the (Cr, Fe) and Ga sublattices is confirmed by the presence of the 111 superlattice diffraction and the ordering of the Co sublattice is identified by the presence of the 200 superlattice diffraction. The observed intensities of the superlattice diffractions are in accord with the calculated ones. With increasing x, the intensity of the 200 diffraction increases and that of the 111 diffraction decreases, showing the substitution effect of Fe for Cr. These superlattice diffractions are also confirmed by electron diffractions.[26] Therefore, it is said that the $L2_1$-type ordered structure is obtained in the entire concentration range of x, different from the case of $Co_2(Cr_{1-x}Fe_x)Al$ alloy system.[15] The room temperature lattice constants a for $x=1.00$ (a), 0.40 (b), and 0.0 (c) are 0.5741, 0.5757, and 0.5765 nm, respectively, consistent with available data.[13] In the XRD pattern of (d), several extra peaks due to the precipitates are observed. The existence of the precipitates is clearly shown in the microstructural observations as discussed below.

The optical micrographs are shown in Figs. 2(a) and 2(b) for the alloy with $x=0.0$ quenched from 1373 K, and annealed at 973 K for 1 week after quenching, respectively. It is confirmed that (a) is in the single phase state, on the contrary, many precipitates are clearly observed in (b). From our previous systematic investigations for the ternary phase diagram of Co-Cr-Ga system,[27] it was disclosed that the single phase of $B2$ exists above 1073 K for the alloy with $x=0.0$, and ε ($A3$-type) and σ ($D8_b$-type) phases coexist with the $L2_1$-phase below 1073 K.

Figure 3 shows the magnetization curves at 4.2 K for the $L2_1$-type $Co_2(Cr_{1-x}Fe_x)Ga$ alloys with $x=0.0$, 0.25, 0.50,

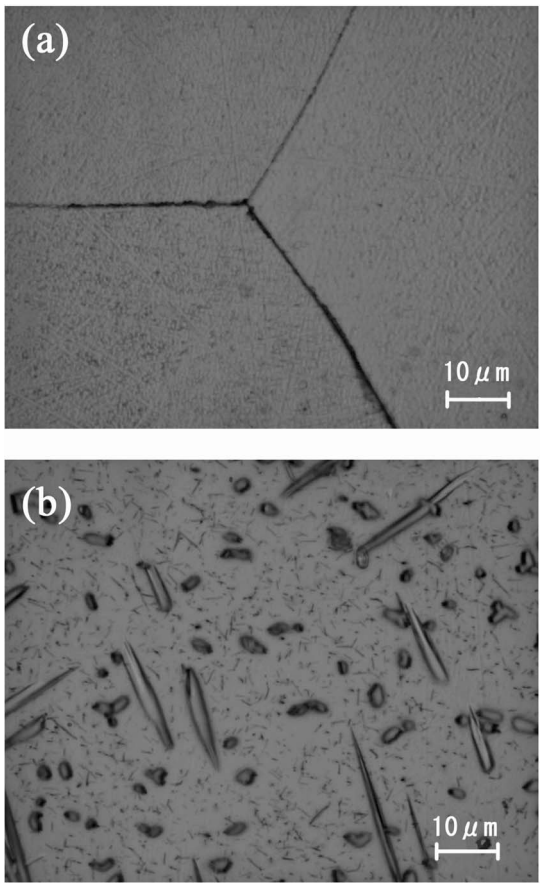

FIG. 2. Optical micrographs of $x=0.0$ ($\equiv Co_2CrGa$), (a) quenched from 1373 K, and (b) annealed at 973 K for 1 week after quenching from 1373 K.

0.60, 0.80, and 1.00. The saturation magnetic moment M_s for $x=0.0$ ($\equiv Co_2CrGa$) alloy is $3.01\mu_B$/f.u., in accord with the generalized Slater-Pauling line, that is, $M_t=Z_t-24$. Here, M_t and Z_t represent the total spin magnetic moment per formula unit and the total number of valence electrons, respectively.[5,28] For the Co_2CrGa alloy, the total number of

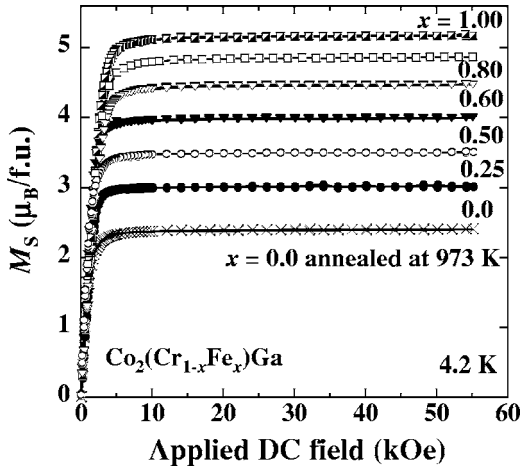

FIG. 3. Magnetization curves at 4.2 K for the $L2_1$-type $Co_2(Cr_{1-x}Fe_x)Ga$ alloys obtained by quenched from 1373 K, together with that for $x=0.0$ annealed at 973 K.

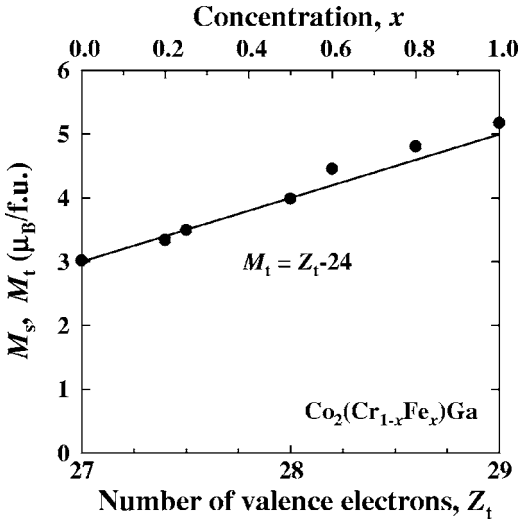

FIG. 4. The saturation magnetic moment at 4.2 K M_s and the total spin magnetic moment M_t obtained from the generalized Slater-Pauling line for the $L2_1$-type $Co_2(Cr_{1-x}Fe_x)Ga$ alloy system as a function of the number of the valence electrons Z_t. The corresponding concentration x is also given in the upper x axis.

valence electrons is 27, and hence the total spin magnetic moment is calculated to be 3. The curve for $x=0.0$ annealed at 973 K for 1 week is also given in the same figure. The value of M_s is obtained to be $2.40\mu_B$/f.u., significantly lower than the theoretical value. It is reasonable that the reduction of M_s comes from the coexistence of precipitates in the present annealed specimen. The ternary phase diagram[27] tells us that the single phase of the stoichiometric composition is not equilibrium state below 1073 K. In this connection, the magnetic state of the σ-phase of CoCr alloy is paramagnetic[29] and the magnetic moment of the ferromagnetic ε-phase is smaller than that of the $L2_1$-type Co_2CrGa alloy.[30]

The saturation magnetic moment M_s for the $L2_1$-type $Co_2(Cr_{1-x}Fe_x)Ga$ alloy system as a function of the number of the valence electrons is plotted in Fig. 4, together with the total spin magnetic moment M_t obtained from the generalized Slater-Pauling line; $M_t=Z_t-24$. In the figure, the corresponding concentration is also given in the upper x axis. In the concentration range below $x=0.50$, M_s increases linearly with increasing x, and then slightly deviates from the generalized Slater-Pauling line above $x=0.60$. For $x=1.00$, the value of M_s is about $5.17\mu_B$/f.u., larger than the expected value of $5\mu_B$/f.u. from the generalized Slater-Pauling line. A similar larger value of M_s for the $L2_1$-type ordered Co_2FeGa alloy has also been reported by several authors.[13,31,32] One may notice that the $L2_1$-type ordered Co_2FeGa alloy is out of accord with half-metallic ferromagnets[31,32] and its electronic structures and the spin polarization ratio will be discussed in connection with Figs. 7 and 8. In order to discuss the larger value of M_s, the effects of the disordering of atoms on the magnetic moments should be taken into account. However, it is unnecessary in the present case because the value of M_s of the $B2$-type disordered phase is slightly lower than that of the value of $L2_1$-type ordered one. Furthermore, if the disordering between the Co and (Cr, Fe) sites occurs, the total

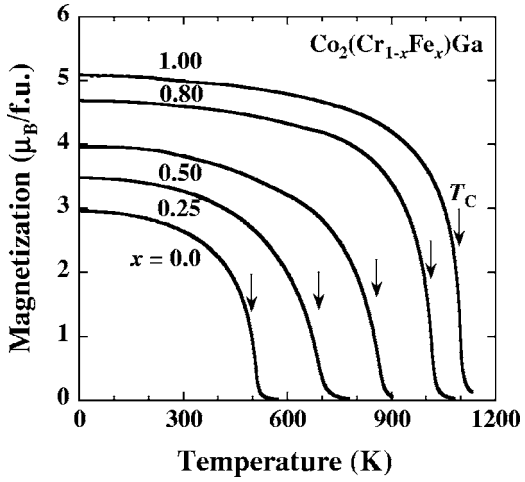

FIG. 5. Temperature dependence of the magnetization measured in a magnetic field of 0.5 T for the $L2_1$-type $Co_2(Cr_{1-x}Fe_x)Ga$ alloys. The arrows indicate the Curie temperature T_C.

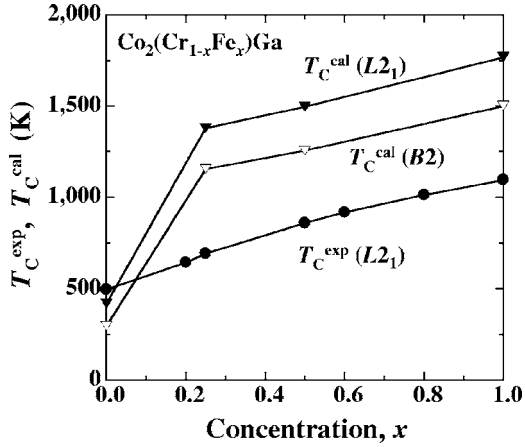

FIG. 6. Concentration dependence of the Curie temperature T_C^{exp} obtained from the temperature dependence of magnetization and the DSC curves (Ref. 26), together with the calculated Curie temperature T_C^{cal} for the $L2_1$- and $B2$-type phases of $Co_2(Cr_{1-x}Fe_x)Ga$ alloy system.

magnetic moment should be reduced. From theoretical investigations for $Co_2(Cr_{0.6}Fe_{0.4})Al$ alloy, it has been reported that the total magnetic moment decreases with proceeding the disordering between the Co and (Cr, Fe) sites.[11] In addition, it has been pointed out that the displacement of atoms between Co and (Cr, Fe) sites is energetically hard. That is, the total energy per unit cell for the alloy having a displacement of 1/5 of Cr into the Co site is about 0.25 eV higher than that of the $L2_1$-type ordered Co_2CrAl alloy.[12] In addition, the magnetic moment is reduced to about $2.6\mu_B$/f.u. when such displacement occurs. Therefore, we should give another explanation for the present larger values of M_s of the $L2_1$-type ordered $Co_2(Cr_{1-x}Fe_x)Ga$ alloys above $x=0.6$.

Recent theoretical studies of the spin-orbit coupling for the Heusler alloys have pointed out that the orbital magnetic moments are negligibly small[33,34] because of a high symmetry of the cubic lattice of Heusler alloys, accompanied by no large magnetic anisotropy. In the $Co_2(Cr_{1-x}Fe_x)Al$ alloy system, however, it has been reported from magnetic circular dichroism (MCD) measurements that the orbital magnetic moments of Co atom for $x=0.40$ and 1.00 are about 10% and 14% of its spin magnetic moment, respectively.[35,36] In addition, in several Co-based Heusler alloy systems, it has also been reported from the MCD measurements that the magnitude of the orbital magnetic moment is about 5%–10% of the spin magnetic moment.[31,37] Therefore, it is expected that the present large value of the magnetic moment would be explained by taking the contribution from the orbital magnetic moment into consideration.

Figure 5 shows the temperature dependence of magnetization measured in a magnetic field of 0.5 T for the $L2_1$-type $Co_2(Cr_{1-x}Fe_x)Ga$ alloys. In the figure, the arrows indicate the Curie temperature T_C obtained from the DSC measurements. The value of T_C increases with increasing x and about 1093 K for $x=1.00$ ($\equiv Co_2FeGa$). The concentration dependence of the Curie temperature determined from the DSC curves T_C^{exp} is shown in Fig. 6, together with the calculated T_C for $L2_1$-type T_C^{cal} ($L2_1$) and $B2$-type T_C^{cal} ($B2$) phases obtained from the effective exchange constant J_0 using Eqs. (1) and (2) in the MFA scheme. Although the value of T_C^{cal} tends to be overestimated because of the MFA, the concentration dependence of T_C is qualitatively in accord with the experimental results T_C^{exp}. That is, the value of T_C^{cal} is higher than T_C^{exp}, except for the value at $x=0$. As discussed below, the magnetic moment of Fe is about twice, comparing with that of Cr, and hence the substitution of Fe for Cr significantly enhances the ferromagnetic interaction. Comparing the $L2_1$- and $B2$-type phases for T_C^{cal} in Fig. 6, the value of T_C^{cal} ($L2_1$) is higher than that of T_C^{cal} ($B2$). For the $Co_2(Cr_{1-x}Fe_x)Al$ alloy system, it has also been pointed out from the Korringa-Kohn-Rostoger (KKR) method with the coherent potential approximation that the energy difference between the ferromagnetic state and the nonmagnetic state for the $L2_1$-type phase is larger than that of the $B2$-type phase.[12] Both of the $L2_1$ and the $B2$-type phases can be obtained after an appropriate heat treatment in the concentration range above $x=0.70$ in $Co_2(Cr_{1-x}Fe_x)Al$ alloy system.[15] In our previous work, we tried to investigate the difference between T_C in the $L2_1$- and the $B2$-type phases of $Co_2(Cr_{1-x}Fe_x)Al$. Unfortunately, T_C of $B2$-type phase cannot be obtained because the $B2$-type phase transforms into the $L2_1$-type phase in the heating process for the thermomagnetization curves. In making processes of films, a metastable state is often obtained. For example, it has been reported that the crystal structure of the films with a high spin polarization ratio for $Co_2(Cr_{1-x}Fe_x)Al$ (Ref. 14) and Co_2MnAl (Ref. 38) is identified as the $B2$-type phase. Therefore, the theoretical calculations for the $B2$-type phase of $Co_2(Cr_{1-x}Fe_x)Ga$ alloy system is also meaningful for practical applications.

The density of states of the $Co_2(Cr_{1-x}Fe_x)Ga$ ($x=0.0$, 0.25, 0.50, and 1.00) alloys are illustrated in Fig. 7. The left- and right-hand panels exhibit the DOSs for the $L2_1$-type (a)–(d) and the $B2$-type phases (a′)–(d′), respectively. The upper and lower curves in each panel correspond to the majority and the minority spin states, respectively. For the calculations for the DOSs for the $B2$-type phase, the coherent potential approximation was adopted. For the $L2_1$-type phase

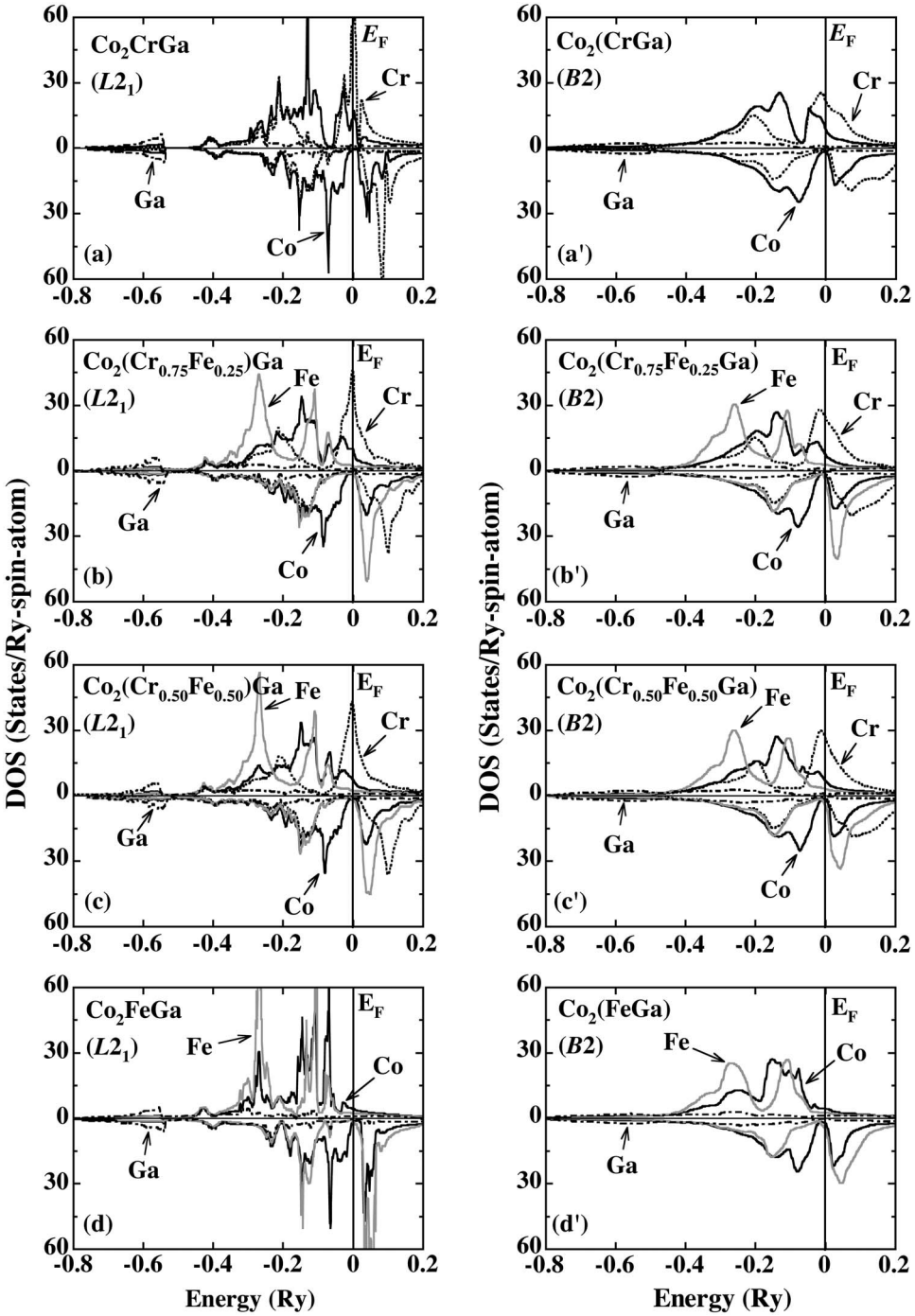

FIG. 7. Density of states of the $Co_2(Cr_{1-x}Fe_x)Ga$ (x=0.0, 0.25, 0.50, and 1.00) alloys. The left- and right-hand panels set out the DOSs for the $L2_1$- and $B2$-type phases, respectively. The upper and lower curves in each panel stand for the majority and the minority spin states, respectively.

from (a) to (d), the large peak of Cr at the Fermi energy E_F observed in the majority spin state decreases with increasing x, in addition, the peak of Co at E_F in the majority spin state moves to an energy region below E_F. As a result, the total DOSs at E_F in the majority spin states for x=1.00 ($\equiv Co_2FeGa$) is relatively low. Furthermore, a large peak of Fe in the minority spin states is found to be close to E_F, being about 0.05 Ry above E_F. It is noted that E_F is not located in the gap but the edge of the peak. As pointed out from other theoretical studies for $L2_1$-type Co_2FeGa alloy by Zhang *et al.*[32] and Deb *et al.*,[39] this effect is due to strong hybridization between the Co-3d and Fe-3d, resulting in a marked reduction of the spin polarization ratio P for Co_2FeGa alloy. A similar substitution effect of Fe on the DOSs is also observed in the $B2$-type phase of $Co_2(Cr_{1-x}Fe_x)Ga$ alloy system. In other words, the half-metallic properties are also kept in the $B2$-type phase in lower concentration range of x. This implies that the character of DOSs is dominated regardless of the order of Co atoms, similar to the $Co_2(Cr_{1-x}Fe_x)Al$ alloy system, in which the systematic theoretical calculations have been carried out,[11,12] and pointed out that the disordering between the Al and the (Cr, Fe) sites scarcely degrades the value of P. On the other hand, the disordering between the Co and the (Cr, Fe) sites brings about a significant reduction of the value of P.[11,12] The calculated values of magnetic moment of each

TABLE I. The calculated values of the magnetic moment of each atom M^{cal} (μ_B/atom), total spin magnetic moment M_t^{cal} (μ_B/f.u.), spin polarization ratio P (%), and the experimental value of the saturation magnetic moment at 4.2 K M_s (μ_B/f.u.), together with the calculated and experimental Curie temperatures T_C^{cal} and T_C^{exp} (K) of the $L2_1$- and $B2$-type phases of the $Co_2(Cr_{1-x}Fe_x)Ga$ alloys.

x	Phase	M_{Co}^{cal} (μ_B/atom)	M_{Cr}^{cal} (μ_B/atom)	M_{Fe}^{cal} (μ_B/atom)	M_{Ga}^{cal} (μ_B/atom)	M_t^{cal} (μ_B/f.u.)	P (%)	M_s (μ_B/f.u.)	T_C^{cal} (K)	T_C^{exp} (K)
0.00	$L2_1$	0.901	1.283		−0.074	3.011	95	3.01	419	495
	$B2$	0.823	1.437		−0.058	3.025	84		295	
0.25	$L2_1$	0.909	1.364	2.764	−0.067	3.466	90	3.49	1378	692
	$B2$	0.896	1.380	2.740	−0.067	3.445	79		1153	
0.50	$L2_1$	1.018	1.375	2.733	−0.068	4.023	85	3.98	1495	858
	$B2$	0.986	1.386	2.728	−0.069	3.960	65		1256	
1.00	$L2_1$	1.187		2.762	−0.095	5.042	37	5.17	1767	1093
	$B2$	1.105		2.722	−0.085	4.847	26		1501	

atom M^{cal} (μ_B/atom), total spin magnetic moment M_t^{cal} (μ_B/f.u.) and spin polarization ratio P (%), the experimental values of the saturation magnetic moment at 4.2 K M_s (μ_B/f.u.), the calculated and experimental Curie temperatures T_C^{cal} and T_C^{exp} (K) of the $Co_2(Cr_{1-x}Fe_x)Ga$ alloys for the $L2_1$- and $B2$-type phases are listed in Table I. The present theoretical values of the magnetic moment of Co and Fe for the $L2_1$-type Co_2FeGa alloy are $1.187\mu_B$ and $2.762\mu_B$, respectively, in agreement with the reported theoretical values of $1.20\mu_B$ and $2.66\mu_B$.[39] Note that the magnetic moment of Fe is much larger than that of bcc Fe and the magnetic moment of Co increases with x.

Shown in Fig. 8 is the concentration dependence of the spin polarization ratio P (%) defined from Eq. (3) for the $L2_1$- and $B2$-type $Co_2(Cr_{1-x}Fe_x)Ga$ alloy systems obtained from the present band calculations. As shown in the figures and the table, the value of P becomes smaller with increasing x, and the value of $B2$-type phase is lower than that of the $L2_1$-type phase in the entire concentration range of x. Especially, in higher concentration of x, the difference between P in both the phases becomes significant. For $x=1.00$ ($\equiv Co_2FeGa$), the ratio of P for the $L2_1$-type phase is 37%, resulting in a remarkable reduction of a half-metallic property in a similar manner as the reported results.[32,39] For practical applications, the half-metallic ferromagnets having a high spin polarization ratio P with a high Curie temperature T_C are highly desired. Accordingly, high values of the spin polarization ratio and the Curie temperature are obtainable by adjusting the amount of Fe for Cr in the $Co_2(Cr_{1-x}Fe_x)Ga$ alloy system.

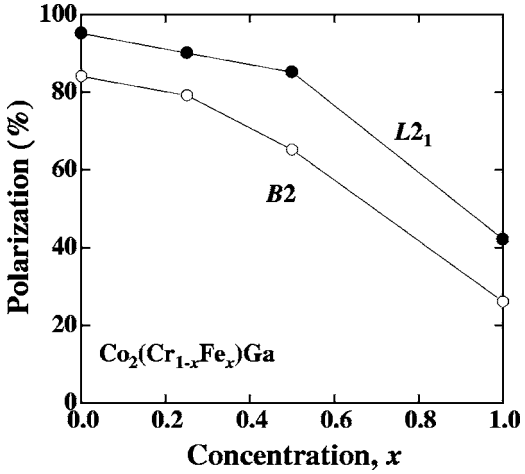

FIG. 8. Concentration dependence of the spin polarization ratio of the $L2_1$- and $B2$-type phases of the $Co_2(Cr_{1-x}Fe_x)Ga$ alloy system.

V. CONCLUSION

In order to investigate the substitution effects of Fe for Cr on the magnetic and half-metallic properties of the $Co_2(Cr_{1-x}Fe_x)Ga$ alloy system, the measurements of the concentration dependence of the saturation magnetic moment and the Curie temperature for the $L2_1$-type phase of $Co_2(Cr_{1-x}Fe_x)Ga$ alloys have been carried out. Next, the density of states, the spin polarization ratio and the effective exchange constant have also been calculated for both the $L2_1$-type and $B2$-type phases. From the present results, it is clear that the Curie temperature T_C of the $L2_1$-type phase of $Co_2(Cr_{1-x}Fe_x)Ga$ alloys increases, whereas the spin polarization ratio P decreases with increasing x. Main results are summarized as follows:

(1) The $L2_1$-type phase is obtained in the entire concentration range by quenching from high temperatures, say 1373 K. For $x=0.0$ ($\equiv Co_2CrGa$), the precipitation is caused by low temperature annealing at 973 K.

(2) The saturation magnetic moment M_s at 4.2 K in lower concentration ranges of x is in good agreement with the theoretical values, following the generalized Slater-Pauling line. The experimental values of M_s in higher concentrations above $x=0.60$ are slightly larger than the theoretical ones.

(3) The Curie temperature T_C increases with increasing x, and its concentration dependence qualitatively agrees with the theoretical results estimated from the effective exchange

constant J_0.

(4) Large ratios of the spin polarization P are obtained not only in the $L2_1$-type phase but also in the $B2$-type phase, although the values of the latter are smaller than those of the former.

(5) The half-metallicity becomes weaker with increasing x, because a large DOS for Cr at E_F in the majority spin band disappears and the gap in the minority spin band becomes narrow due to the hybridization between Fe-3d and Co-3d bands.

---

*Core Research for Evolutional Science and Technology–Japan Science and Technology Agency.

†Corresponding author. Email address: rie@material.tohoku.ac.jp

[1] S. A. Wolf, D. D. Awschalom, R. A. Buhrman, J. M. Daughton, S. von Molnár, M. L. Roukes, A. Y. Chtchelkanova, and D. M. Treger, Science **294**, 1488 (2001).

[2] R. A. de Groot, F. M. Mueller, P. G. van Engen, and K. H. J. Buschow, Phys. Rev. Lett. **50**, 2024 (1983).

[3] S. Ishida, S. Sugimura, S. Fujii, and S. Asano, J. Phys.: Condens. Matter **3**, 5793 (1991).

[4] S. Ishida, S. Fujii, D. Kashiwagi, and S. Asano, J. Phys. Soc. Jpn. **64**, 2152 (1995).

[5] I. Galanakis, P. H. Dederichs, and N. Papanikolaou, Phys. Rev. B **66**, 174429 (2002).

[6] M. P. Raphael, B. Ravel, Q. Huang, M. A. Willard, S. F. Cheng, B. N. Das, R. M. Stroud, K. M. Bussmann, J. H. Claassen, and V. G. Harris, Phys. Rev. B **66**, 104429 (2002).

[7] U. Geiersbach, A. Bergmann, and K. Westerholt, Thin Solid Films **425**, 225 (2003).

[8] K. Inomata, S. Okamura, and N. Tezuka, J. Magn. Magn. Mater. **282**, 269 (2004).

[9] A. Kellow, N. E. Fenineche, T. Grosdidier, H. Aourag, and C. Coddet, J. Appl. Phys. **94**, 3292 (2003).

[10] S. Ishida, S. Kawakami, and S. Asano, Mater. Trans., JIM **45**, 1065 (2004).

[11] Y. Miura, K. Nagao, and M. Shirai, J. Appl. Phys. **95**, 7225 (2004).

[12] Y. Miura, K. Nagao, and M. Shirai, Phys. Rev. B **69**, 144413 (2004).

[13] K. H. J. Buschow and P. G. van Engen, J. Magn. Magn. Mater. **25**, 90 (1981).

[14] S. Okamura, R. Goto, N. Tezuka, S. Sugimoto, and K. Inomata, Jpn. J. Appl. Phys., Part 1 **28**, 172 (2004).

[15] K. Kobayashi, R. Y. Umetsu, R. Kainuma, K. Ishida, T. Oyamada, R. Kainuma, K. Ishida, R. Y. Umetsu, A. Fujita, and K. Fukamichi, Appl. Phys. Lett. **85**, 4684 (2004).

[16] I. Ohnuma, R. Kainuma, and K. Ishida (unpublished).

[17] R. Y. Umetsu, K. Kobayashi, R. Kainuma, A. Fujita, K. Fukamichi, K. Ishida, and A. Sakuma, Appl. Phys. Lett. **85**, 2011 (2004).

[18] V. Ja. Markiv and V. G. Rachinskij, Dopov. Akad. Nauk. Ukr. RSR, Ser. A: Fiz.-Mat. Tekh. Nauki **40**, 278 (1978).

[19] K. Ishikawa, M. Ise, I. Ohnuma, R. Kainuma, and K. Ishida, Ber. Bunsenges. Phys. Chem. **102**, 1206 (1998).

[20] O. K. Andersen, Phys. Rev. B **12**, 3060 (1975).

[21] U. von Barth and L. Hedin, J. Phys. C **5**, 1629 (1972).

[22] J. F. Janak, Solid State Commun. **25**, 53 (1978).

[23] A. Sakuma, J. Phys. Soc. Jpn. **69**, 3072 (2000).

[24] A. I. Liechtenstein, M. I. Katsneson, and V. A. Gubanov, Solid State Commun. **54**, 327 (1985).

[25] J. M. D. Coey and M. Venkatesan, J. Appl. Phys. **91**, 8345 (2002).

[26] K. Kobayashi, R. Y. Umetsua, A. Fujita, K. Oikawa, R. Kainuma, K. Fukamichi, and K. Ishida, J. Alloys Compd. **399**, 60 (2005).

[27] K. Kobayashi, R. Kainuma, K. Fukamichi, and K. Ishida, J. Alloys Compd. **403**, 161 (2005).

[28] J. Kübler, Physica B & C **127**, 257 (1984).

[29] N. Môri and T. Mitsui, J. Phys. Soc. Jpn. **26**, 1087 (1969).

[30] K. H. J. Buschow, P. G. van Engen, and R. Jungebreur, J. Magn. Magn. Mater. **38**, 1 (1983).

[31] P. J. Brown, K. U. Neumann, P. J. Webster, and K. R. A. Ziebeck, J. Phys.: Condens. Matter **12**, 1827 (2000).

[32] M. Zhang, E. Brück1, F. R. de Boer, Z. Li, and G. Wu, J. Phys. D **37**, 2049 (2004).

[33] S. Picozzi, A. Continenza, and A. J. Freeman, Phys. Rev. B **66**, 094421 (2002).

[34] I. Galanakis, Phys. Rev. B **71**, 012413 (2005).

[35] H. J. Elmers, S. Wurmehl, G. H. Fecher, G. Jakob, C. Felser, and G. Schönhense, J. Magn. Magn. Mater. **272–276**, 758 (2004).

[36] H. J. Elmers, S. Wurmehl, G. H. Fecher, G. Jakob, C. Felser, and G. Schönhense, Appl. Phys. A **79**, 557 (2004).

[37] A. Yamasaki, S. Imada, R. Arai, H. Utsunomiya, S. Suga, T. Muro, Y. Saitoh, T. Kanomata, and S. Ishida, Phys. Rev. B **65**, 104410 (2002).

[38] H. Kubota, J. Nakata, M. Oogane, Y. Ando, A. Sakuma, and T. Miyazaki, Jpn. J. Appl. Phys., Part 2 **43**, L984 (2004).

[39] A. Deb, M. Itou, Y. Sakurai, N. Hiraoka, and N. Sakai, Phys. Rev. B **63**, 064409 (2001).